minerals

MDPI

Article

The Removal of Uranium and Thorium from Their Aqueous Solutions by 8-Hydroxyquinoline Immobilized Bentonite

Bahaa A. Salah *, Mohamed S. Gaber and Abdel hakim T. Kandil

Chemistry Department, Faculty of Science, Helwan University, Ain Helwan, Helwan 11795, Egypt; ms4435900@gmail.com (M.S.G.); abdelhakimkandil@gmail.com (A.h.T.K.)

* Correspondence: BAHAA_HUSSEIN@science.helwan.edu.eg

Received: 10 September 2019; Accepted: 6 October 2019; Published: 11 October 2019

Abstract: The sorption of uranium and thorium from their aqueous solutions by using 8-hydroxyquinoline modified Na-bentonite (HQ-bentonite) was investigated by the batch technique. Na-bentonite and HQ-bentonite were characterized by X-ray fluorescence (XRF), X-ray diffraction (XRD), scanning electron microscopy (SEM), and Fourier Transform Infrared (FTIR) spectroscopy. Factors that influence the sorption of uranium and thorium onto HQ-bentonite such as solution pH, contact time, initial metal ions concentration, HQ-bentonite mass, and temperature were tested. Sorption experiments were expressed by Freundlich and Langmuir isotherms and the sorption results demonstrated that the sorption of uranium and thorium onto HQ-bentonite correlated better with the Langmuir isotherm than the Freundlich isotherm. Kinetics studies showed that the sorption followed the pseudo-second-order kinetic model. Thermodynamic parameters such as ΔH°, ΔS°, and ΔG° indicated that the sorption of uranium and thorium onto HQ-bentonite was endothermic, feasible, spontaneous, and physical in nature. The maximum adsorption capacities of HQ-bentonite were calculated from the Langmuir isotherm at 303 K and were found to be 63.90 and 65.44 for U(VI) and Th(IV) metal ions, respectively.

Keywords: sorption; uranium; thorium; bentonite; adsorption kinetics; Langmuir isotherm

1. Introduction

Removal of radioactive and hazardous metal ions from wastewater is a pivotal issue in the treatment of liquid waste because these ions are extremely dangerous to the human health and the environment due to their high chemical toxicity, even at low concentrations and their long half-lives [1]. Exposure to radioactive ions may cause damage to biological systems, such as kidney damage, toxic hepatitis, histopathological system damage, skin corrosion, and even cancer [2]. These radioactive wastes appear in water from processes producing nuclear fuels and from various industrial activities such as nuclear power plants, mining, nuclear weapons, nuclear armament, and laboratories working with radioactive materials [3]. Hazardous pollutants are removed by several techniques such as chromatographic extraction, membrane dialysis, flotation, ion exchange [4], chemical precipitation [5,6], solvent extraction [7,8], nanofiltration [9], biological processes [10], and adsorption processes [11]. However, most of these techniques are expensive and not efficient in the removal of low metal ion concentrations. Due to the high advantages of adsorption processes like low cost, simple selectivity, high efficiency, easy operation, [12], and rapid kinetics [13], it becomes a suitable technique for the removal of hazardous metal ions from wastewater.

Various sorbents have been used for the removal of radioactive metal ions [14]; among them, clay minerals have received much attention because of their abundance, low cost, and high sorption

capacity [15]. Bentonite is a natural clay mineral consists of one central alumina octahedral sheet (AlO_6) sandwiched between two silica tetrahedral sheets (SiO_4). The negative charge on the bentonite surface is a consequence of the isomorphous substitution of Si^{4+} with Al^{3+} and Al^{3+} with Mg^{2+} in the tetrahedral and octahedral layers, respectively, which entails charge balance between this negative charge and the exchangeable cations on the layer surfaces such as Na^{+} and Ca^{2+} [16]. Bentonite has some physicochemical properties such as accessibility, low cost, chemical composition, surface acidity, high cation exchange capacity, crystallinity of its smectite, large specific surface area, strong adsorptive affinity for inorganic and organic pollutants, low permeability, and ubiquitous presence in most soils [2,17]. Recently, several researches have been devoted to bentonite modification, in order to further enhance its sorption efficiency [18]. Complexing agent such as 8-hydroxyquinoline has been widely used in analytical chemistry for separation and pre-concentration of heavy metal ions [19]. Immobilization of bentonite by 8-hydroxyquinoline gives an efficient sorbent, 8-hydroxyquinoline modified Na-bentonite (HQ-bentonite), that was applied for the retention of heavy metal ions such as Pb(II), Cd(II), and Cu(II) [12,19,20]. To date, however, few studies on the removal of radioactive metal ions by using HQ-bentonite have been reported.

The present study aimed to explore the applicability of 8-hydroxyquinoline modified Na-bentonite for the removal of U(VI) and Th(IV) ions from their aqueous solutions. The influences of various experimental conditions such as dose of adsorbent, initial concentration of each metal ion, contact time, solution pH, and temperature were investigated. Sorption isotherm models have been examined in terms of Freundlich and Langmuir equations. Sorption kinetics and Thermodynamic parameters such as ΔH°, ΔS°, and ΔG°, were evaluated and interpreted.

2. Materials and Methods

2.1. Reagents

All the chemicals used in this study were of analytical grade and used without further purification. All reagent preparations were done in a fume cupboard. The stock solution (1000 mg/L) of U(VI) and Th(IV) ions was prepared from $UO_2(NO_3)_2{\cdot}6H_2O$ and $Th(NO_3)_4{\cdot}5H_2O$ (Riedel-De Haen AG, Germany), by dissolving 2.11 g and 2.48 g, respectively, in 1 L (acidified with 2 mL HNO_3) of deionized water. Working solutions of U(VI) and Th(IV) ions were prepared from the stock solution by appropriate dilution.

2.2. Adsorbent

In this study, Na-bentonite was supplied by Research-Lab Fine Chem Industries (Mumbai, India). The cation exchange capacity (CEC) was determined by using the methylene blue method [21], and it was found as 0.900 mmol/g. Na-bentonite was immobilized by 8-hydroxyquinoline (Sigma-Aldrich, St. Louis, MO, USA, 99% purity) according to the reported method [20].

2.3. Characterization

X-ray fluorescence, (Panalytical Axios Advanced, The Netherlands), was used to identify the chemical constituents of the samples. The constituents' phases of samples were identified by an X-ray diffraction analysis (Brucker AXS D8 advance, Karlsruche, Germany) with CuKα radiation (λ = 1.5406 Å). All the samples were scanned from 2° to 70° at 2θ range, step size (0.02°) and step time (0.4 s). Quanta FEG-250 scanning electron microscope (FEI Corporate, Hillsboro, OR, USA) analysis with accelerating voltage 30 kV, magnification up to 100,000 X was used to illustrate the sample morphology. The vibration spectrum (400–4000 cm^{-1}) of the samples was measured by Spectrum Two Perkin Elmer Fourier Transform Infrared (FT-IR) spectrometer (PerkinElmer, Inc., Waltham, MA, USA) using the ATR technique. The pH measurements were obtained by Jenco 6173 model (Shanghai Jenco Instruments Co., Shanghai, China). UV-Vis spectrophotometer (Jasco V-630, Jasco Corporation, Tokyo, Japan) (±0.005 A), was used for all spectrophotometric determinations.

2.4. Batch Adsorption Experiments

The adsorption of U(VI) and Th(IV) ions onto HQ-bentonite was tested as a function of sorbent mass, solution pH, uranium and thorium ion initial concentrations, contact time, and temperature. In the experiments, HQ-bentonite was suspended in 50 mL solution of uranium and thorium at different experimental conditions and pH range (1–9) ± 0.1 (adjusted with 0.1 mol/L NaOH and 0.1 mol/L HNO_3). After equilibrium, the solution was separated from the solid by centrifugation at 4000 rpm for 10 min. Afterward, the residual U(VI) and Th(IV) ions in aqueous solution were analyzed and determined spectrophotometrically using the Arsenazo III method with a spectrophotometer at a maximum wavelength of 650 and 656 nm, respectively, against reagent blank [22]. The difference between the initial and equilibrium concentration was used to calculate the amount of metal ions taken up by the sorbent. The sorption percentage (%), distribution parameter (K_d, L/g), and sorption amount (q_e, mg/g) of U(VI) and Th(IV) ions adsorbed onto HQ-bentonite were calculated using Equations (1)–(3), respectively.

$$Sorption(\%) = \frac{C_o - C_e}{C_o} \times 100 \quad (1)$$

$$k_d = \left(\frac{C_o - C_e}{C_e}\right)\frac{v}{m} \quad (2)$$

$$q_e = (C_o - C_e)\frac{v}{m} \quad (3)$$

where, C_o and C_e are the initial and equilibrium concentrations of metal ions in the solution (mg/L), respectively, V is the volume of the solution (L), m is the mass of dry sorbent in grams, and q_e is the adsorption capacity of sorbent (mg/g).

2.5. Desorption Studies

Desorption is a reverse process of adsorption from which the target metal ions can be recovered and the spent adsorbent can be regenerated and reused [23]. In this study, different reagents such as NaCl, HNO_3, and HCl, at different concentrations ranging from 0.05 to 0.25 M, were used as stripping agents for the determination of desorption properties of HQ-bentonite. Masses of 0.1 g of U(VI) and Th(IV) ions loaded HQ-bentonite were placed in 50 mL of the stripping agent under the shaking time of 15 min at room temperature. After the experiment, the eluted adsorbate was filtered and analyzed to estimate U(VI) and Th(IV) ion concentrations. The striping percentage was calculated using Equation (4).

$$Striping(\%) = \frac{C}{C_o} \times 100 \quad (4)$$

where C is the concentration (mg/L) of the metal ion in the eluting agent after a proper time and C_o (mg/L) is the concentration of the metal ion on the adsorbent material surface (mg/L).

3. Results and Discussion

3.1. Characterization

3.1.1. Chemical Composition of Na-Bentonite and HQ-Bentonite

The chemical constituents of Na-bentonite and HQ-bentonite (Table 1) indicate the presence of alumina and silica as major components along with traces of magnesium, potassium, iron, titanium, and calcium oxides [12]. The mass percentage of Na_2O decreased after the modification of Na-bentonite; this indicates that the exchange took place between the 8-hydroxyquinoline and the sodium ions of the Na-bentonite.

Table 1. The chemical constituents of Na-bentonite and HQ-bentonite.

Constituents	Mass%	
	Na-Bentonite	HQ-Bentonite
Na_2O	4.616	0.504
SiO_2	46.75	44.57
Al_2O_3	19.86	17.86
$Fe_2O_3{}^{total}$	12.23	11.74
MgO	1.947	1.515
CaO	1.019	0.311
TiO_2	2.152	2.017
P_2O_5	0.123	0.089
K_2O	1.055	0.934
SO_3	0.289	0.033
Loss of ignition (Loi)	8.700	19.70

3.1.2. X-ray Diffraction (XRD) Analysis

The XRD pattern of Na-bentonite (Figure 1) demonstrated a d_{001} peak at 12.953 Å, whereas that of HQ-bentonite is at 15.857 Å. The expansion in the basal spacing of the Na-bentonite was calculated as 2.904 Å. This indicated an immobilization of the chelating species in the interlayer space of the Na-bentonite [12]. These results are in line with the scanning electron microscopy (SEM) results in this study.

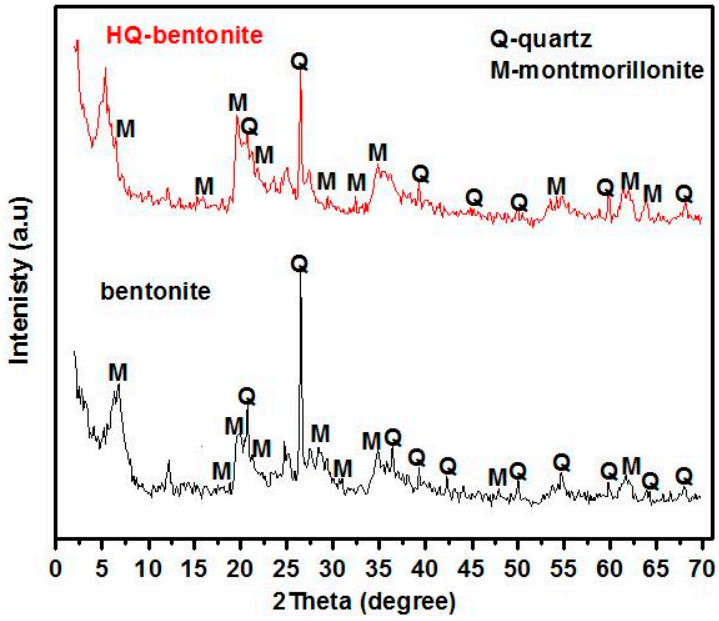

Figure 1. X-ray diffraction (XRD) analysis of Na-bentonite and HQ-bentonite.

3.1.3. SEM Images and EDX Analysis

The surface morphology and microstructure of Na-bentonite, HQ-bentonite, and U(VI) and Th(IV) ions loaded HQ-bentonite are shown in Figures 2–4. Results indicated that the surface morphology of Na-bentonite is relatively smoother, and reveals a more spongy appearance with irregular structure than HQ-bentonite. After modification, HQ-bentonite surfaces became swollen and accompanied by a small number of holes. This swelling indicated that 8-hydroxyquinoline intercalated into the inner layers of Na-bentonite. To compare the altering of surface morphology and trace the elemental changes after the adsorption, SEM and EDX micrographs of U(VI) and Th(IV) ions loaded HQ-bentonite

(Figures 3 and 4) were measured. After loading with U(VI) and Th(IV) ions, the HQ-bentonite structure was covered with the encaged ions. This provided complementary evidence for the adsorption process.

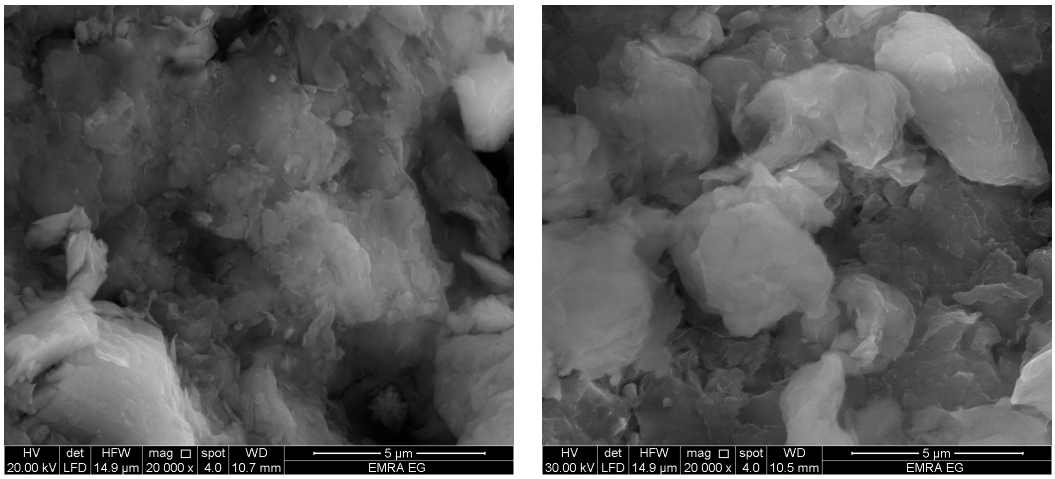

(**a**) (**b**)

Figure 2. Scanning electron microscopy (SEM) images of (**a**) Na-bentonite and (**b**) HQ-bentonite.

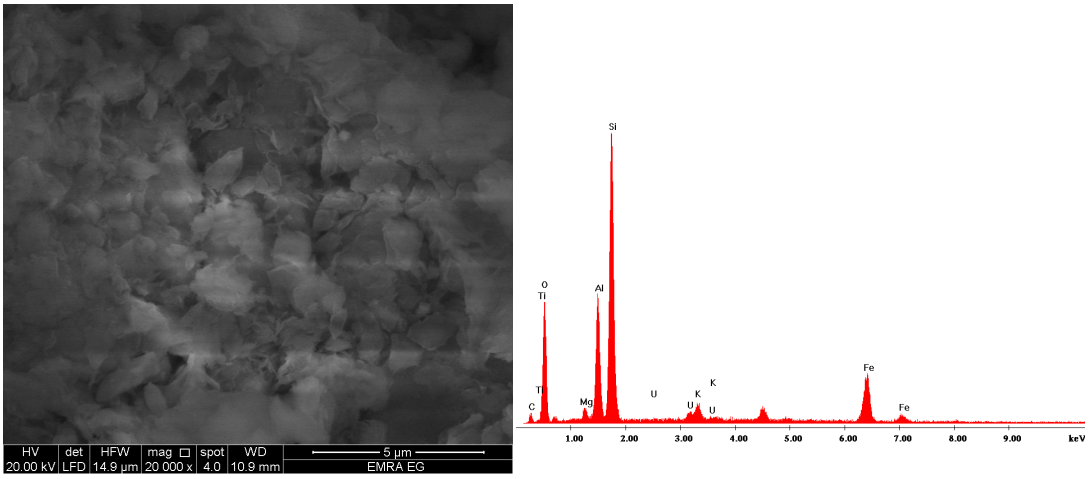

Figure 3. SEM images and EDX of U(VI) ions loaded HQ-bentonite.

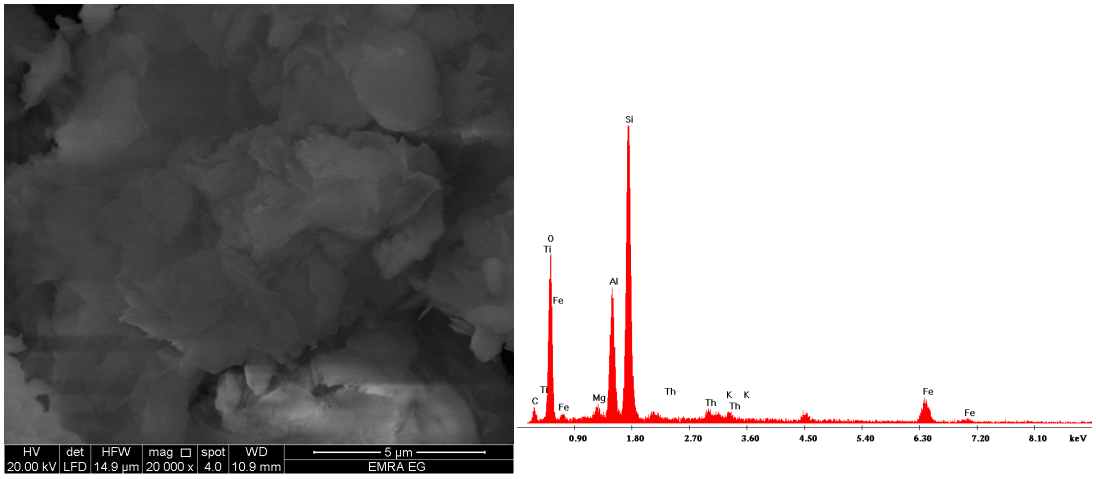

Figure 4. SEM images and EDX of and Th(IV) ions loaded HQ-bentonite.

3.1.4. FT-IR Spectrograms

Figure 5a–d demonstrates the FT-IR spectra of Na-bentonite, HQ-bentonite, and U(VI) and Th(IV) ions loaded HQ-bentonite, respectively. The figure gives information on the intercalation of the 8-hydroxyquinoline onto the Na-bentonite and the interaction nature of HQ-bentonite with metal ions. Na-bentonite shows (Figure 5a) an absorption peak at 3620 cm^{-1} which is attributed to (O–H) stretching vibration of the silanol (Si–OH) group. The strong band at 1000 cm^{-1} is due to the (Si–O–Si) groups of the tetrahedral sheet. The deep peak at 912 cm^{-1} shows the stretching vibration of (Al–Al–OH). The band at 798 cm^{-1} is attributed to quartz in the sample. The stretching vibration band at 693 cm^{-1} is ascribed to the deformation and bending modes of the Si–O bond. The bands at 466 and 524 cm^{-1} are attributed to (Si–O–Si) and (Al–O–Si) bending vibrations, respectively. The (C–C) and (C–N) ring stretching (skeletal) vibrations in the HQ-bentonite (Figure 5b) are located at 1604, 1500, 1466, 1381, and 1322 cm^{-1} and the ring bending vibration are obtained at 825 cm^{-1} but these bands were not observed in the Na-bentonite [12]. This gives acceptable proof for the intercalation of 8-hydroxyquinoline onto Na-bentonite. As shown in Figure 5c,d after the adsorption of U(VI) and Th(IV) onto HQ-bentonite, the observed shifts were as follow: the (O–H)stretching vibration of the silanol (Si–OH) group was shifted to 3621 $cm^{-1,}$ the (Si–O–Si) band of the tetrahedral sheet was shifted to 1007 cm^{-1} and the stretching vibration of (Al–Al–OH) was shifted to 913 cm^{-1}, for both metal ions. The C–C and C–N ring stretching bands were moved to 1380 and 1308 cm^{-1} for U(VI) and 1738, 1420, 1378, and 1313 cm^{-1} for Th(IV), whereas, the ring bending vibration was shifted to 817 cm^{-1} for U(VI) and 800 cm^{-1} for Th(IV). The deformation and bending bands of the Si–O bond were shifted to 693 and 692 cm^{-1} for U(VI) and Th(IV), respectively. The bending vibrations band of Si–O–Si was moved to 467 $cm^{-1,}$ whereas, the Al–O–Si was shifted to 527 cm^{-1}, for both metal ions. These peak shifts indicate the interaction between the metal ions and HQ-bentonite.

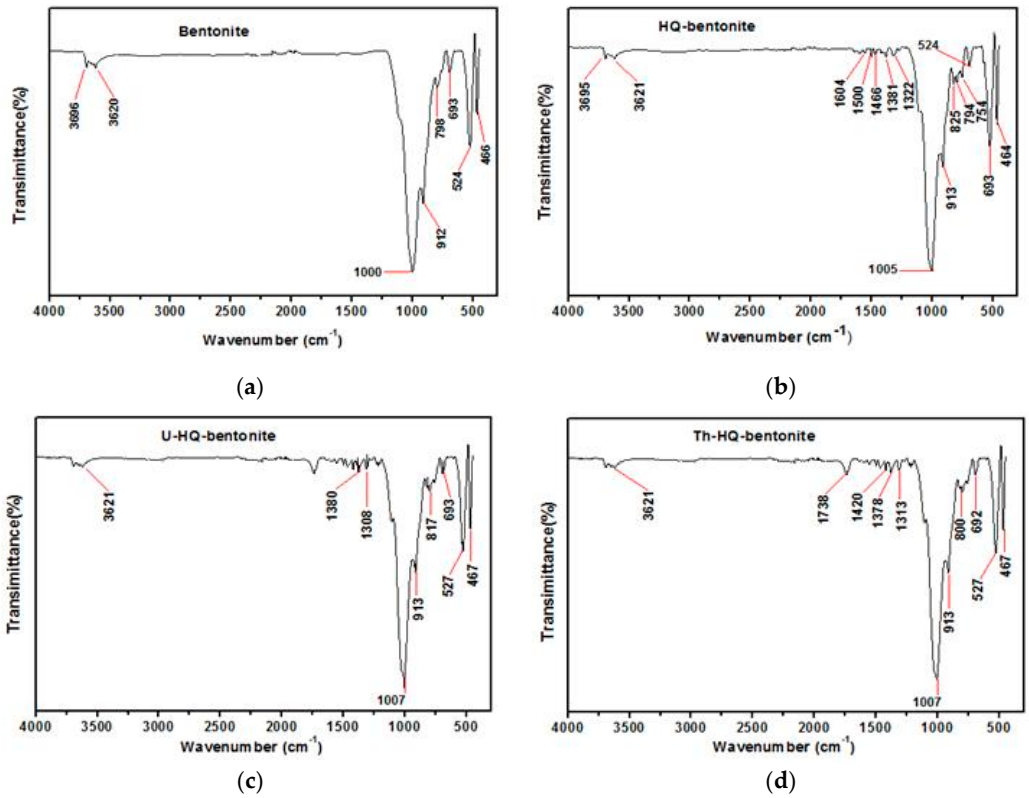

Figure 5. Fourier Transform Infrared (FT-IR) spectra of (**a**) Na-bentonite, (**b**) HQ-bentonite, (**c**) U(VI) ions loaded HQ-bentonite, and (**d**) Th(IV) ions loaded HQ-bentonite.

3.1.5. Effect of Contact Time

Figure 6 shows the influence of shaking time on U(VI) and Th(IV) sorption onto HQ-bentonite. From the figure, it is clear that the uptake percentage of U(VI) and Th(IV) ions increased rapidly with increasing contact time till reaching equilibrium at 15 and 8 min. of shaking for U(VI) and Th(IV), respectively, then remaining constant.

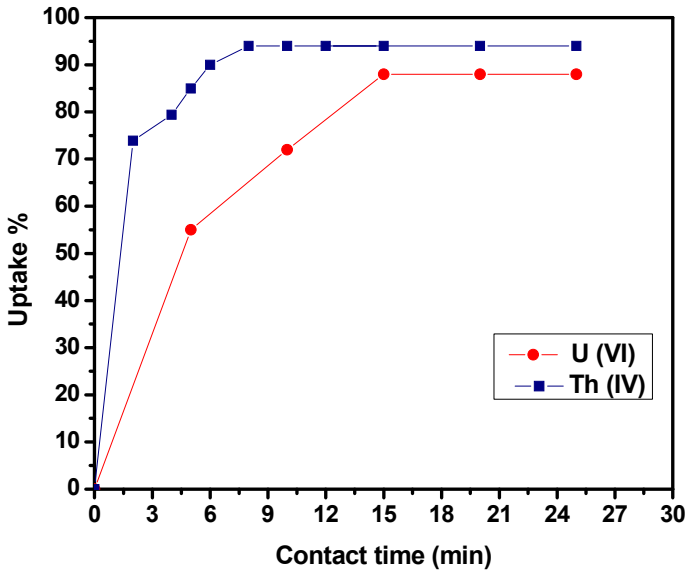

Figure 6. Effect of contact time on U(VI) and Th(IV) ions sorption onto HQ-bentonite. Conditions: 0.1 g HQ-bentonite; 50 mL solution; 100 mg/L metal ion; U(VI) (pH, 4), Th(IV) (pH, 3); temperature 303 K.

3.1.6. Effect of Initial pH

The pH of the aqueous solution is the most important parameter that influences the adsorption of metal ions. The solution pH can alter not only surface binding sites but also surface charge and metal speciation. It was reported that HQ-bentonite has no point of zero charge(pH_{pzc}), and it exhibits negative zeta potential and negative surface charge at pH values ranging from 2 to 9 [12].

Figure 7 shows the effect of initial pH on U(VI) and Th(IV) sorption onto HQ-bentonite. The results illustrate that at high acidity, competition between U(VI) (or Th(IV)) and dominant H_3O^+ ions towards the active adsorption sites took place. This reduced the adsorption efficiency of metal ions. By increasing the pH values, more active sites were exposed to metal ions and hence adsorption efficiency increased reaching maximum at pH 4 for both metal ions.

It should be mentioned that the species distribution in solution for both metal ions varies by varying the pH values. At pH values less than 3, UO_2^{2+} ions exist as the predominant species [24]. At pH 4, hydrolysis of the uranyl ions commences; where mononuclear $[UO_2(OH)]^+$ as well as polynuclear species such as $[(UO_2)_2(OH)_2]^{2+}$ and $[(UO_2)_3(OH)_5]^+$ are formed. The little adsorptive affinity of these species accounts for the decrease in U(VI) removal efficiency at pH values above 4 [25,26]. Similarly, Th(IV) speciation varies by altering the pH values. At pH values less than 3, Th^{4+} ions exist as the major species. At pH values beyond 4, the hydrolysis products as well as the precipitation begin to play a role in the adsorption of Th(IV) [27,28]; so, the uptake percentage maintains constancy with increasing pH above 4.0. To avoid precipitation, a solution pH of 3 and 4 for Th(IV) and U(VI) was used for further experiments [3].

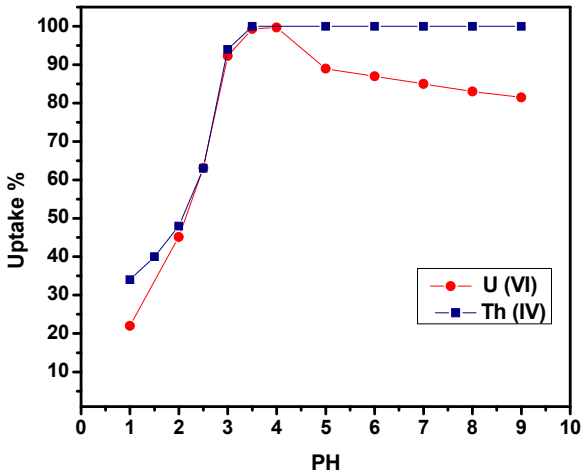

Figure 7. Effect of pH on U(VI) and Th(IV) ions sorption onto HQ-bentonite. Conditions: 0.1 g HQ-bentonite; 50 mL solution; 100 mg/L metal ion; shaking time U(VI) (15 min), Th(IV) (8 min); temperature 303 K.

3.1.7. Effect of the Initial Concentration of Metal Ions

The influence of the initial concentration of U(VI) and Th(IV) on uptake percentage of HQ-bentonite is shown in Figure 8. The results showed a decrease in the uptake percentage by increasing the initial concentration of metal ions. The poor adsorption capacity at high metal ion concentrations is attributed to the increased ratio of sorption quantity of U(VI) and Th(IV) ions on the HQ-bentonite surface to available vacant sites.

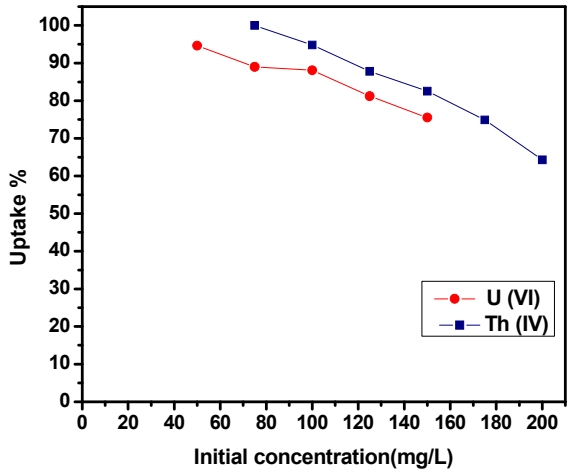

Figure 8. Effect of metal ions initial concentration on U(VI) and Th(IV) ions sorption onto HQ-bentonite. Conditions: 0.1 g HQ-bentonite; 50 mL solution; U(VI) (pH 4), Th(IV) (pH 3); shaking time U(VI) (15 min.), Th(IV) (8 min.); temperature 303 K.

3.1.8. Effect of Sorbent Mass

Figure 9 illustrates the effect of sorbent mass on the adsorption of U(VI) and Th(IV) onto HQ-bentonite. The results revealed that as the amount of sorbent increased, the sorption of U(VI) and Th(IV) increased due to increasing the number of sorbent particles in the solution which led to the interaction of more metal ions with more binding sites till this became constant at 0.15 g for both metal ions.

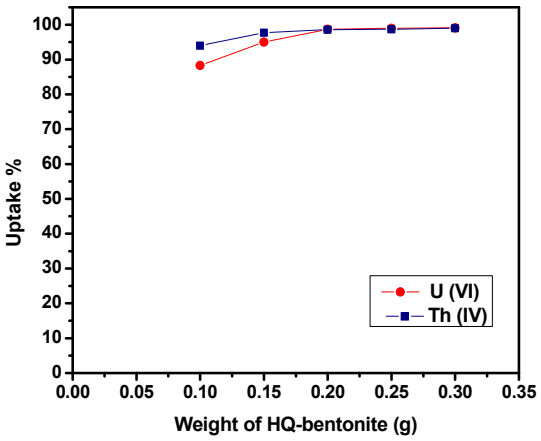

Figure 9. Effect of adsorbent mass on U(VI) and Th(IV) ions sorption onto HQ-bentonite. Conditions: 100 mg/L metal ion; 50 mL solution; U(VI) (pH 4), Th(IV) (pH 3); shaking time U(VI) (15 min.), Th(IV) (8 min.); temperature = 303 K.

3.1.9. Effect of Temperature

The effect of temperature on the sorption of U(VI) and Th(IV) metal ions onto HQ-bentonite was studied. As illustrated in Figure 10 with increasing the temperature, the number of reacting moles having excess energy increased, this led to an increase in the uptake percentage of U(VI) and Th(IV) ions, so the sorption rate and the rate of mass transfer of the diffusion was increased.

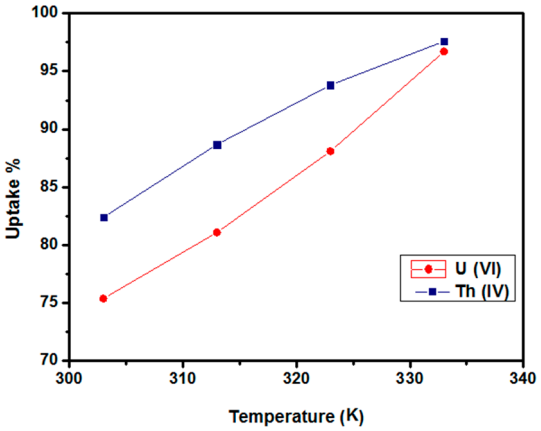

Figure 10. Effect of temperature on U(VI) and Th(IV) ions sorption onto HQ-bentonite. Conditions: 0.1g HQ-bentonite; 150 mg/L metal ion; 50 mL solution; U(VI) (pH 4), Th(IV) (pH 3); shaking time U(IV) (15 min.), Th(IV) (8 min.).

3.1.10. Comparison of the Sorption Efficiency of HQ-Bentonite with Na-Bentonite

In order to demonstrate the potential enhancements to U(VI) and Th(IV) removal offered by HQ-bentonite over Na-bentonite, the sorption optimum conditions (0.1 g adsorbent; 100 mg/L metal ion; 50 mL solution; U(VI) (pH 4), Th(IV) (pH 3); shaking time U(IV) (15 min.), Th(IV) (8 min.); 303 K) were tested using Na-bentonite. It was found that the uptake% values decreased from 88% to 14% and from 95% to 19%, for U(VI) and Th(IV), respectively.

3.2. Sorption Isotherms

The adsorption isotherm is the relationship between the adsorption capacity and the residual concentration at equilibrium at constant temperature [29]. The adsorption isotherm explains the distribution of the adsorbed molecules between the solid and liquid phases at equilibrium. Freundlich and Langmuir isotherms are the most frequently used models for analyzing adsorption equilibrium data.

3.2.1. Freundlich Adsorption Isotherm

The Freundlich isotherm model is suitable for heterogeneous surface energy systems. It postulates that the sorption takes place with a heterogeneous distribution of energetically active sites, where there is interaction among adsorbates on the adsorbent surfaces. The Freundlich equation can be described by the linearized equation (Equation (5)) [12].

$$Log\ q_e = \log k + \frac{1}{n} \log C_e \tag{5}$$

where C_e is the equilibrium concentration of adsorbate in solution (mg/L), q_e is the equilibrium adsorption capacity (mg/g), k and n are system-specific constants, Log k is an indicator of sorption capacity, and $1/n$ is a measure of intensity of adsorption. When Log q_e is plotted against log C_e, the slope and the intercept of the straight line gives $\frac{1}{n}$ and log k, respectively.

Table 2 shows the values of Freundlich isotherm parameters. The deviation from the linearity was estimated from the value of n. If the value of n is equal to unity, this indicates that the sorption process is a chemical process [3]. From Table 2, the values of n for U (VI) and Th (IV) are above unity. This indicates that the adsorption of U(VI) and Th(IV) on HQ-bentonite is a favorable physical process. The values of the linear correlation coefficient (R^2) showed that the Freundlich isotherm model does not fit the sorption of U(VI) and Th (IV) onto HQ-bentonite.

Table 2. Isotherms parameters and values of linear correlation factors (R^2) for sorption of U(VI) and Th(IV) ions onto HQ-bentonite.

Metal Ion	Freundlich Isotherm			Langmuir Isotherm		
	n	**Log *K***	R^2	Q_e **(mg/g)**	***b*** **(L/mg)**	R^2
U(VI)	3	1.235	0.9517	63.90	0.168	0.9881
Th(IV)	8.7	1.603	0.8320	65.44	0.640	0.9988

3.2.2. Langmuir Adsorption Isotherm

The Langmuir model adopts that the uptake of adsorbates takes place on homogeneous surfaces where all the adsorption sites are energetically identical. In addition, only a saturated monolayer of adsorbates is formed with no interaction among them on the plane of the adsorbent surface.

The Langmuir equation can be expressed by the linearized equation (Equation (6)) [12].

$$\frac{C_e}{q_e} = \frac{1}{bQ_e} + \frac{C_e}{Q_e} \tag{6}$$

where C_e is the equilibrium concentration of adsorbate in solution (mg/L), q_e is the equilibrium adsorption capacity (mg/g), Q_e (mg/g) is the maximum adsorption capacity, and b (L/mg) is Langmuir constant related to the free energy of sorption. Figure 11 shows the plot of $\frac{Ce}{qe}$ versus Ce. The slope and the intercept of the regression line give $\frac{1}{Qe}$ and $\frac{1}{b\ Qe}$, respectively. Langmuir isotherm parameters with correlation coefficients were evaluated and are presented in Table 2. The linear form of the plot over the entire concentration indicates the applicability of the Langmuir model to the sorption of U(VI) and Th(IV) onto HQ-bentonite. The Langmuir equilibrium parameter R_L is expressed as in Equation (7) [12].

$$R_L = \frac{1}{(1 + bC_o)} \tag{7}$$

where C_o is the initial concentration of metal ions (mg/L) and b (L/mg) is Langmuir constant related to the free energy of sorption. The value of R_L explains the nature of adsorption isotherm to be favorable ($0 < R_L < 1$), unfavorable ($R_L > 1$), linear ($R_L = 1$), or irreversible ($R_L = 0$) [30]. Calculated data reveal

that the R_L value was found to be 0.039 and 0.0078 for U(VI) and Th(IV) ions, respectively, this indicates that the adsorption of the U(VI) and Th(IV) onto HQ-bentonite is favorable.

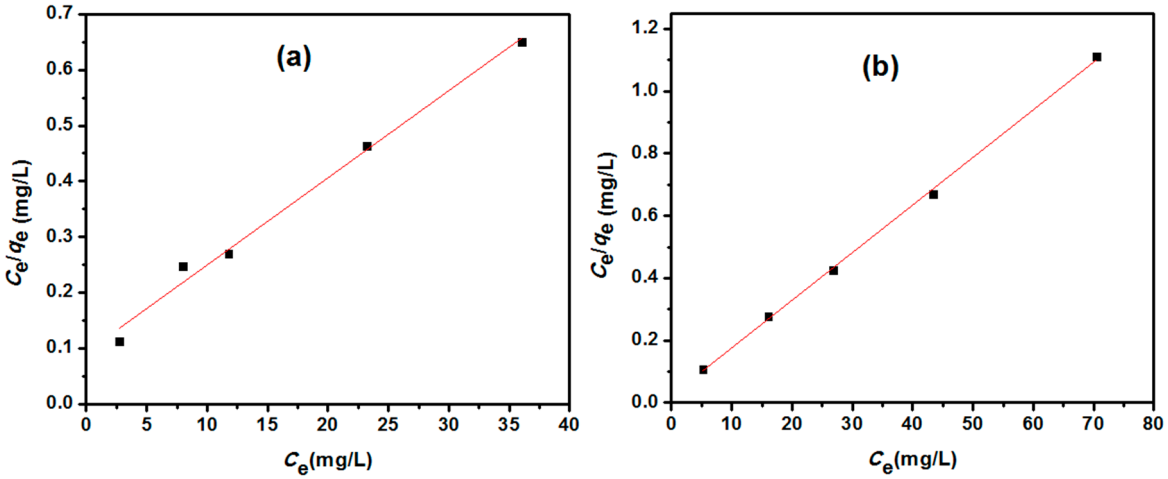

Figure 11. Langmuir sorption isotherm of (**a**) U(VI) and (**b**) Th(IV) sorption onto HQ-bentonite. Conditions: 0.1 g HQ-bentonite; 50 mL solution; U(VI) (pH 4), Th(IV) (pH 3); shaking time U(VI) (15 min.), Th(IV) (8 min.); temperature 303 K.

3.3. Sorption Kinetics

The adsorption kinetics explains the relationship between the adsorption rate and the adsorption time in the adsorption process; the pseudo-first-order and pseudo-second-order models were used to explain the kinetic characteristic of U(VI) and Th(IV) onto HQ-bentonite. The pseudo-first-order model is expressed as the following equation [31].

$$Log(q_e - q_t) = \log q_e - \left(\frac{k_1 t}{2.303}\right) \quad (8)$$

the pseudo-second-order model is described as the following equation [31].

$$\left(\frac{t}{q_t}\right) = \left(\frac{1}{k_2 q_e^2}\right) + \left(\frac{t}{q_e}\right) \quad (9)$$

where q_e and q_t (mg/g) are the amount of metal ion adsorbed at equilibrium and time t, respectively, and k_1 and k_2 are the equilibrium rate constant (min^{-1}) of the pseudo-first-order and pseudo-second-order adsorption, respectively. Using Equation (8), the linear form of log ($q_e - q_t$) versus t was plotted. Figure 12 shows the linear plot of t/q_t versus t using Equation (9).

Table 3 shows the calculated values of k, q_e, E_a, and correlation coefficient (R^2) of the pseudo-first- and pseudo-second-order models for U(VI) and Th(IV) ions sorption on HQ-bentonite. The results reveal that the pseudo-second-order kinetic model fits the data for the sorption process since the values of the correlation coefficient (R^2) of pseudo-second-order were higher than the value of the pseudo-first-order model. The natural logarithms of the rate constant (K) were used according to the Arrhenius equation to calculate the activation energy of the sorption process. A plot of log k versus $1/t$ gives a straight line as shown in Figures 13 and 14. The activation energy for pseudo-first-order and pseudo-second-order can be calculated from the slope of the line since the slope is equal to ($\frac{-Ea}{2.303\ R}$). The calculated values of activation energy of U(VI) and Th(IV) onto HQ-bentonite were found as 13.7 and 17 kJ/mol for uranium and thorium, respectively (Table 3), which are within the activation energy range 0–40 kJ/mol, indicating that the adsorption of U(VI) and Th(IV) onto HQ-bentonite is a physical one [30,32].

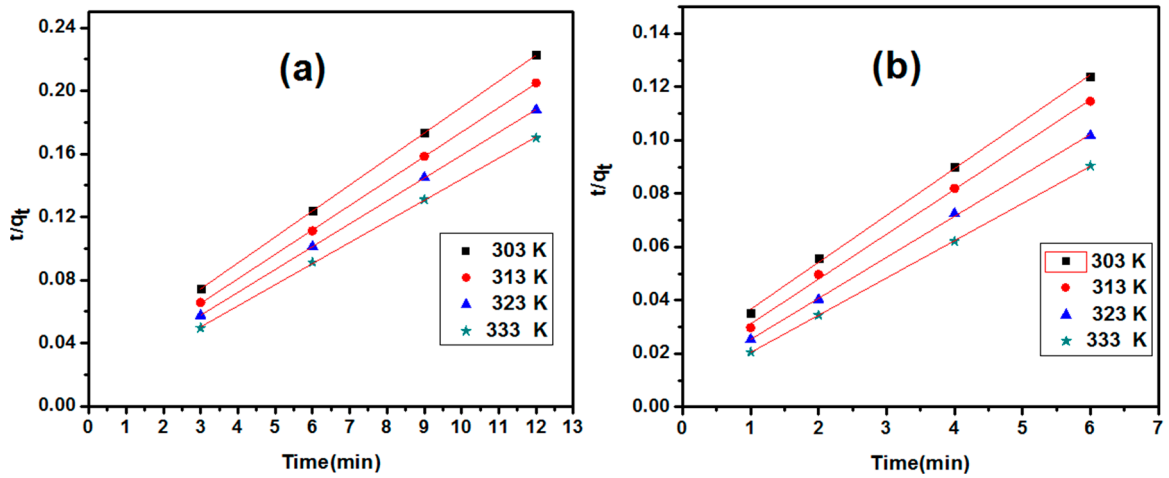

Figure 12. Plot of t/q_t versus time for (**a**) U(VI) and (**b**) Th(IV) sorption onto HQ-bentonite. Conditions: 0.1g HQ-bentonite; 150 mg/L metal ion; 50 mL solution; U(VI) (pH 4), Th(IV) (pH 3).

Table 3. Adsorption kinetics parameters of the pseudo-first-order model and pseudo-second-order model for U(VI) and Th(IV) sorption onto HQ-bentonite at different temperatures.

Metal Ion	Temperature	Pseudo-First-Order				Pseudo-Second-Order			
	(*k*)	K_1 (min^{-1})	q_e	R^2	E_{a1} (kJ/mol)	$K_2 \times 10^{-3}$ (g/mg·min)	q_e	R^2	E_{a2} (kJ/mol)
U(VI)	303	0.217	29.3	0.9977		10.9	60.7	1	
	313	0.229	27.5	0.9922		12.8	64.5	0.9999	
	323	0.226	25.7	0.9964	0.8	14.9	68.9	0.9999	13.7
	333	0.225	23.4	0.9929		17.8	74.6	0.9997	
Th(IV)	303	0.133	45	0.9596		16.2	56.9	0.998	
	313	0.128	43	0.9573		19.7	59.5	0.998	
	323	0.135	39.8	0.9006	4.4	23.6	65.1	0.999	17
	333	0.155	33.3	0.8630		30.1	71.6	0.999	

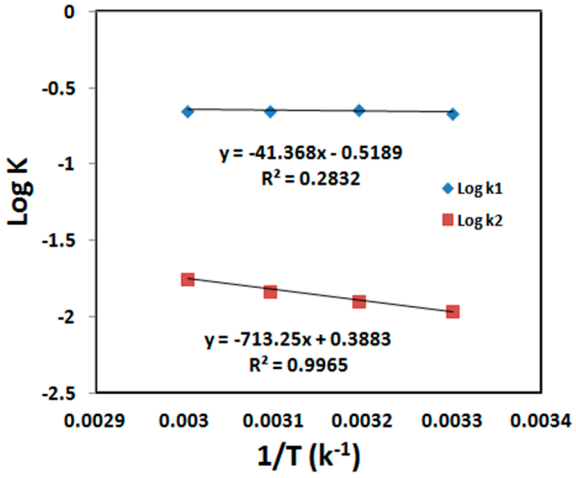

Figure 13. Variation of log k_1 and log k_2 with $1/T$ for sorption of U(VI) onto HQ-bentonite (Arrhenius plot).

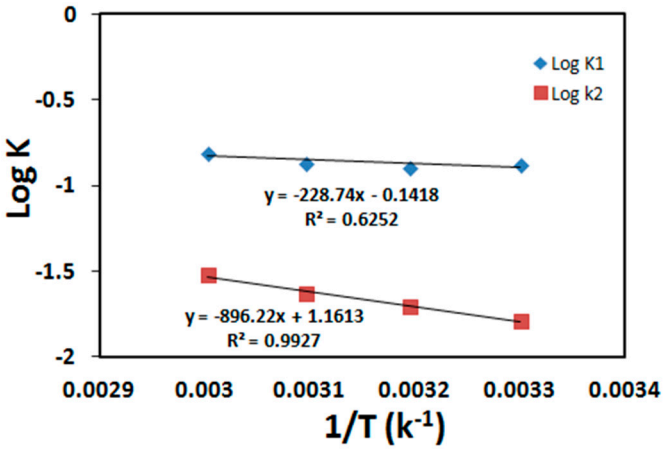

Figure 14. Variation of log k_1 and log k_2 with $1/T$ for sorption of Th(IV) onto HQ-bentonite (Arrhenius plot).

3.4. Thermodynamic Parameters

Thermodynamic parameters such as $\Delta G°$, $\Delta H°$, and $\Delta S°$ are used to indicate whether the particular adsorption process is physical or chemical, spontaneous or non-spontaneous, and also exothermic or endothermic. Thermodynamic parameters were calculated by using Equations (10) and (11) [31].

$$\ln k_D = \frac{\Delta S^\circ}{R} - \frac{\Delta H^\circ}{RT} \tag{10}$$

$$\Delta G^\circ = \Delta H^\circ - T\Delta S^\circ \tag{11}$$

where $\Delta H°$, $\Delta S°$, and $\Delta G°$ are the standard enthalpy, entropy, and Gibbs free energy (kJ/mol·K), respectively. K_D is the distribution coefficient (L/g), T is the absolute temperature (K), and R is the gas constant (8.314 J/mol·K).

The values of enthalpy change ($\Delta H°$) and entropy change ($\Delta S°$) can be calculated from the slope and intercept of the plot of ln K_D versus $1/T$ (Figure 15). On the other hand values of $\Delta G°$ at various temperatures were calculated from Equation (11). The values of $\Delta H°$, $\Delta S°$, and $\Delta G°$ are presented in Table 4. The Gibbs free energy ($\Delta G°$) negative values demonstrate that the adsorption process is spontaneous and feasible. The results show that as the temperature increases, $\Delta G°$ values become more negative which indicates that the adsorption process becomes more spontaneous and efficient, which favors the adsorption process. The enthalpy ($\Delta H°$) positive values imply that the adsorption process is endothermic and physical. The enthalpy positive values are due to metal ions desolvation enthalpy exceeding the sorption enthalpy. The entropy ($\Delta S°$) positive values reflect the increase in randomness at the solid-liquid interface and the affinity of HQ-bentonite towards U(VI) and Th(IV). The thermodynamic parameters' values imply that the sorption process is entropy driven.

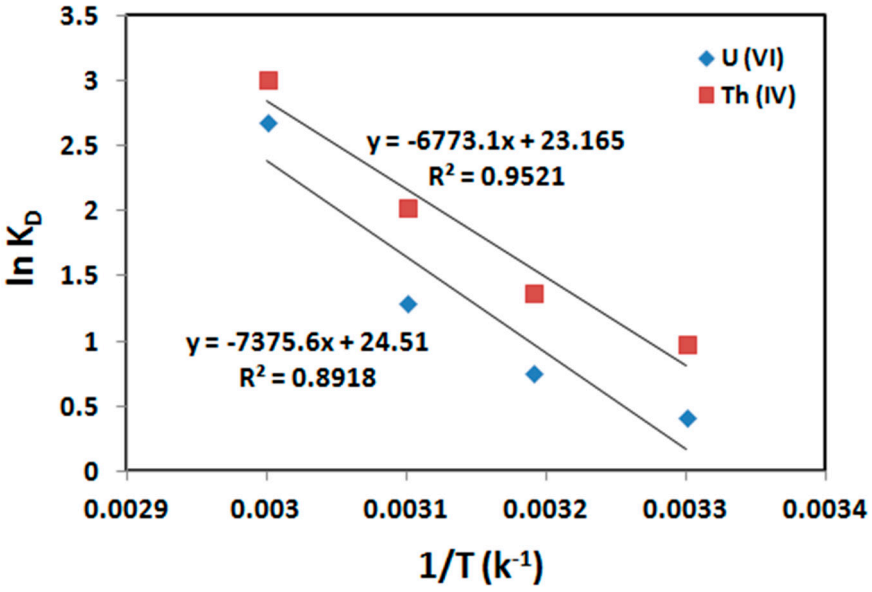

Figure 15. Variation of ln K_D with 1/T for sorption of U(VI) and Th(IV) onto HQ-bentonite.

Table 4. Values of thermodynamic parameters of U(VI) and Th(IV) ions sorption onto HQ-bentonite.

Metal Ion	ΔH° (kJ/mol)	ΔS° (kJ/mol K)	ΔG° (kJ/mol)			
			303 K	313 K	323 K	333 K
U(VI)	61.3	0.20	−0.70	−1.30	−3.30	−5.30
Th(IV)	56.3	0.19	−1.26	−3.16	−5.06	−6.96

3.5. Desorption Studies

Desorption is one of the most important aspects of the applicability of the adsorbents [33]. It can be seen from Figure 16 that there was a lower stripping percentage using NaCl compared with HCl and HNO_3 and that with increasing the concentrations of stripping agents, the stripping percentage increased.

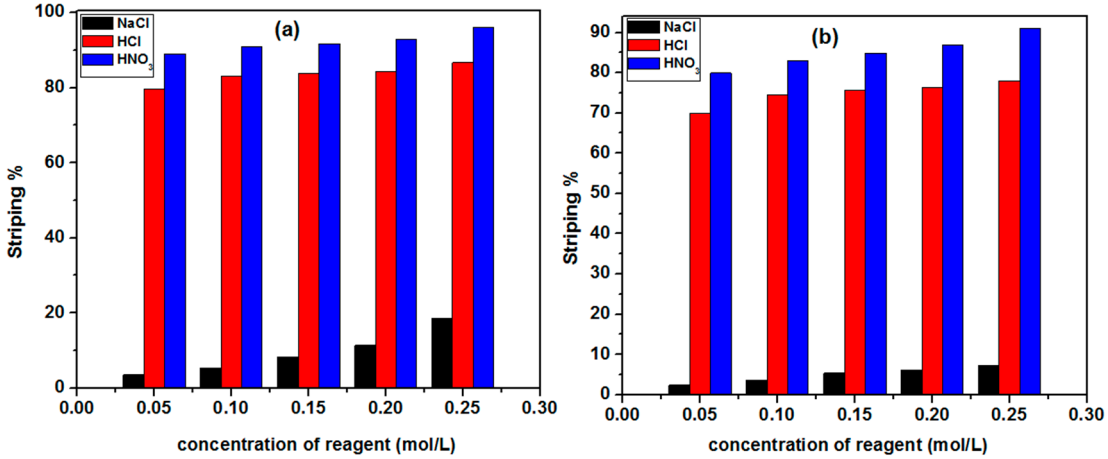

Figure 16. Effect of NaCl, HCl, and HNO_3 on stripping percentage of (**a**) U(VI) and (**b**) Th(IV) from HQ-bentonite.

The regenerated HQ-bentonite was reused up to four cycles using 0.25 M HCl or 0.25 M HNO_3 (Figure 17). The amount of sorbed or desorbed metal ions almost remained constant throughout the four cycles. The slight decrease in the efficiency of adsorbent might be due to the little amount lost

during adsorption-desorption cycles. The obtained results indicated that the adsorption-desorption process onto HQ-bentonite was a reversible process.

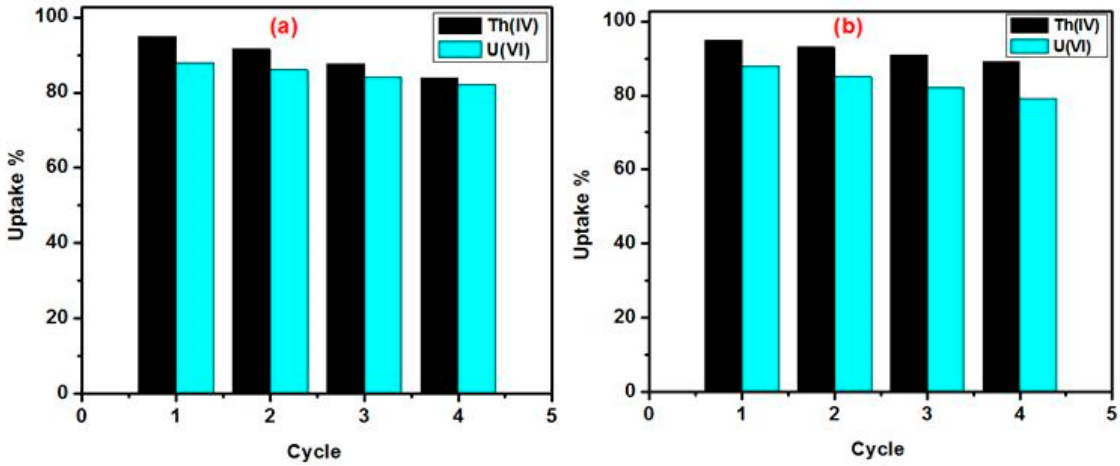

Figure 17. Recycling of U(VI) and Th(IV) loaded HQ-bentonite using (**a**) 0.25 M HCl and (**b**) 0.25 M HNO_3. Sorption conditions: 0.1 g HQ-bentonite; 100 mg/L metal ion; 50 mL solution; U(VI) (pH 4), Th(IV) (pH 3); shaking time U(IV) (15 min.), Th(IV) (8 min.); 303 K.

3.6. Comparison of U(VI) and Th(IV) Sorption Capacity of HQ-bentonite with Other Sorbents

Table 5 shows a comparative assessment for adsorption of U(VI) and Th(IV) with other sorbents. The large sorption capacity of HQ-bentonite, relative to other sorbents, reveals the great potential of HQ-bentonite as an alternative sorbent for removal of U (VI) and Th(IV) from their aqueous solutions.

Table 5. Comparison of the maximum sorption capacity of U (VI) and Th (IV) onto HQ-bentonite with various sorbents at room temperature.

Sorbent	Q_{max} (mg/g)		References
	U(VI)	Th(IV)	
Diatomite (DT) Diatomite-hexadecyltrimethylammonium	26.04	30.30	[3]
(DT-HDTMA)	38.47	46.01	[3]
Insolubilized humic acid	16.95	20.00	[34]
Illite	5.266	7.169	[35,36]
Acid activated Na-bentonite	11.80	14.30	[37,38]
Thermally and chemically modified Na-bentonite	29.60	-	[39]
Na-Bentonite	9.124	11.40	[40,41]
HQ-bentonite	63.90	65.44	This work

4. Conclusions

In this study, Na-bentonite was modified with 8-hydroxyquinoline. The chemical composition, functional groups, and surface microstructure of Na-bentonite and HQ-bentonite were characterized by X-ray fluorescence (XRF), XRD), FTIR), and SEM. Results indicated that the sorption of U(VI) and Th(IV) ions from their aqueous solutions onto HQ-bentonite was greatly influenced by experimental factors as contact time, solution pH, initial concentration of each ion, dose of adsorbent, and temperature. Equilibrium data were analyzed using Freundlich and Langmuir isotherms, sorption data revealed that the adsorption of U(VI) and Th(IV) onto HQ-bentonite was better fitted to the Langmuir adsorption isotherm than the Freundlich model. It was found that the sorption of U(VI) and Th(IV) onto HQ-bentonite followed pseudo-second-order kinetics with activation energy 13.7 and 17 kJ/mole for U(VI) and Th(IV), respectively. The thermodynamic parameters $\Delta G°$, $\Delta S°$, and $\Delta H°$ indicated that the sorption process was spontaneous, feasible, endothermic, and physical in nature. The sorption

capacity of Na-bentonite was greatly enhanced by modifying it with 8-hydroxyquinoline; the maximum adsorption capacity values were found to be 63.90 and 65.44 mg/g for U(VI) and Th(IV), respectively. The desorption study showed that the HQ-bentonite can be reused after elution of U(VI) and Th(IV) ions with 0.25 M HCl or 0.25 $MHNO_3$, up to four cycles. The regeneration use of HQ-bentonite would enhance the economics of adsorption of U(VI) and Th(IV) ions from pollutants. The present study has shown the value of HQ-bentonite as an efficient sorbent for the removal of radioactive metal ions from the wastewater.

Author Contributions: This work is part of the M.Sc. studies of the second author mentioned in the authors' list, M.S.G., under the supervision of the first author, B.A.S.; and the third author, A.h.T.K. A.h.T.K. and B.A.S. have proposed the study plan, participated in data interpretation, results discussion, and revising the written paper. M.S.G. has done the experimental work, participated in results discussion, and written the manuscript.

Funding: This research received no external funding.

Conflicts of Interest: The authors declare no conflict of interest.

References

1. Humelnicu, D.; Dinu, M.V.; Drăgan, E.S. Adsorption characteristics of UO_2^{2+} and Th^{4+} ions from simulated radioactive solutions onto chitosan/clinoptilolite sorbents. *J. Hazard. Mater.* **2011**, *185*, 447–455. [CrossRef] [PubMed]
2. Xiao, J.; Chen, Y.; Zhao, W.; Xu, J. Sorption behavior of U(VI) onto Chinese bentonite: Effect of pH, ionic strength, temperature and humic acid. *J. Mol. Liq.* **2013**, *188*, 178–185. [CrossRef]
3. Salameh, S.I.Y.; Khalili, F.I.; Al-Dujaili, A.H. Removal of U(VI) and Th(IV) from aqueous solutions by organically modified diatomaceous earth: Evaluation of equilibrium, kinetic and thermodynamic data. *Int. J. Miner. Process.* **2017**, *168*, 9–18. [CrossRef]
4. Houhoune, F.; Nibou, D.; Chegrouche, S.; Menacer, S. Behaviour of modified hexadecyltrimethylammonium bromide bentonite toward uranium species. *J. Environ. Chem. Eng.* **2016**, *4*, 3459–3467. [CrossRef]
5. Mellah, A.; Chegrouche, S.; Barkat, M. The precipitation of ammonium uranyl carbonate (AUC): Thermodynamic and kinetic investigations. *Hydrometallurgy* **2007**, *85*, 163–171. [CrossRef]
6. Tyrpekl, V.; Beliš, M.; Wangle, T.; Vleugels, J.; Verwerft, M. Alterations of thorium oxalate morphology by changing elementary precipitation conditions. *J. Nucl. Mater.* **2017**, *493*, 255–263. [CrossRef]
7. Gasser, M.S.; Emam, S.S.; Rizk, S.E.; Salah, B.A.; Sayed, S.A.; Aly, H.F. Extraction and separation of uranium(IV) and certain light lanthanides from concentrated phosphoric acid solutions using octyl phenyl acid phosphate. *J. Mol. Liq.* **2018**, *272*, 1030–1040. [CrossRef]
8. Bayyari, M.A.; Nazal, M.K.; Khalili, F.A. The effect of ionic strength on the extraction of Thorium(IV) from nitrate solution by didodecylphosphoric acid (HDDPA). *J. Saudi Chem. Soc.* **2010**, *14*, 311–315. [CrossRef]
9. Favre-Réguillon, A.; Lebuzit, G.; Murat, D.; Foos, J.; Mansour, C.; Draye, M. Selective removal of dissolved uranium in drinking water by nanofiltration. *Water Res.* **2008**, *42*, 1160–1166. [CrossRef]
10. Sureshkumar, M.K.; Das, D.; Mallia, M.B.; Gupta, P.C. Adsorption of uranium from aqueous solution using chitosan-tripolyphosphate (CTPP) beads. *J. Hazard. Mater.* **2010**, *184*, 65–72. [CrossRef]
11. Aytas, S.; Yurtlu, M.; Donat, R. Adsorption characteristic of U (VI) ion onto thermally activated bentonite. *J. Hazard. Mater.* **2009**, *172*, 667–674. [CrossRef] [PubMed]
12. Özcan, A.S.; Gök, Ö.; Özcan, A. Adsorption of lead(II) ions onto 8-hydroxy quinoline-immobilized bentonite. *J. Hazard. Mater.* **2009**, *161*, 499–509. [CrossRef] [PubMed]
13. Wang, Y.Q.; Zhang, Z.B.; Li, Q.; Liu, Y.H. Adsorption of uranium from aqueous solution using $HDTMA^+$-pillared bentonite: Isotherm, kinetic and thermodynamic aspects. *J. Radioanal. Nucl. Chem.* **2012**, *293*, 231–239. [CrossRef]
14. Kütahyali, C.; Eral, M. Selective adsorption of uranium from aqueous solutions using activated carbon prepared from charcoal by chemical activation. *Sep. Purif. Technol.* **2004**, *40*, 109–114. [CrossRef]
15. Su, J.; Huang, H.G.; Jin, X.Y.; Lu, X.Q.; Chen, Z.L. Synthesis, characterization and kinetic of a surfactant-modified bentonite used to remove As(III) and As(V) from aqueous solution. *J. Hazard. Mater.* **2011**, *185*, 63–70. [CrossRef]

16. Shah, L.A.; da Silva Valenzuela, M.D.G.; Farooq, M.; Khattak, S.A.; Valenzuela Díaz, F.R. Influence of preparation methods on textural properties of purified bentonite. *Appl. Clay Sci.* **2018**, *162*, 155–164. [CrossRef]
17. Ma, J.; Qi, J.; Yao, C.; Cui, B.; Zhang, T.; Li, D. A novel bentonite-based adsorbent for anionic pollutant removal from water. *Chem. Eng. J.* **2012**, *200–202*, 97–103. [CrossRef]
18. Pandey, S.; Ramontja, J. Recent Modifications of bentonite Clay for Adsorption Applications. *Focus Sci.* **2016**, *2*, 1–10. [CrossRef]
19. Bentouami, A.; Ouali, M.S. Cadmium removal from aqueous solutions by hydroxy-8 quinoleine intercalated bentonite. *J. Colloid Interface Sci.* **2006**, *293*, 270–277. [CrossRef]
20. Gök, Ö.; Özcan, A.; Erdem, B.; Özcan, A.S. Prediction of the kinetics, equilibrium and thermodynamic parameters of adsorption of copper(II) ions onto 8-hydroxy quinoline immobilized bentonite. *Colloids Surf. A Physicochem. Eng. Asp.* **2008**, *317*, 174–185. [CrossRef]
21. Kahr, G.; Madsen, F.T. Determination of the cation exchange capacity and the surface area of bentonite, illite and kaolinite by methylene blue adsorption. *Appl. Clay Sci.* **1995**, *9*, 327–336. [CrossRef]
22. Marczenko, Z. *Separation and Spectrophotometric Determination of Elements*; John Wiley & Sons Australia: Hoboken, NJ, USA, 1986; pp. 424–446.
23. Zuo, Q.; Gao, X.; Yang, J.; Zhang, P.; Chen, G.; Li, Y.; Shi, K.; Wu, W. Investigation on the thermal activation of montmorillonite and its application for the removal of U(VI) in aqueous solution. *J. Taiwan Inst. Chem. Eng.* **2017**, *80*, 754–760. [CrossRef]
24. Anirudhan, T.S.; Jalajamony, S. Ethyl thiosemicarbazide intercalated organophilic calcined hydrotalcite as a potential sorbent for the removal of uranium(VI) and thorium(IV) ions from aqueous solutions. *J. Environ. Sci. (China)* **2013**, *25*, 717–725. [CrossRef]
25. Liu, Y.; Li, Q.; Cao, X.; Wang, Y.; Jiang, X.; Li, M.; Hua, M.; Zhang, Z. Removal of uranium(VI) from aqueous solutions by CMK-3 and its polymer composite. *Appl. Surf. Sci.* **2013**, *285*, 258–266. [CrossRef]
26. Zhang, X.; Jiao, C.; Wang, J.; Liu, Q.; Li, R.; Yang, P.; Zhang, M. Removal of uranium(VI) from aqueous solutions by magnetic Schiff base: Kinetic and thermodynamic investigation. *Chem. Eng. J.* **2012**, *198–199*, 412–419. [CrossRef]
27. Cheng, L.; Zhai, L.; Liao, W.; Huang, X.; Niu, B.; Yu, S. An investigation on the behaviors of thorium(IV) adsorption onto chrysotile nanotubes. *J. Environ. Chem. Eng.* **2014**, *2*, 1236–1242. [CrossRef]
28. Talip, Z.; Eral, M.; Hiçsönmez, Ü. Adsorption of thorium from aqueous solutions by perlite. *J. Environ. Radioact.* **2009**, *100*, 139–143. [CrossRef]
29. Du, S.; Wang, L.; Xue, N.; Pei, M.; Sui, W.; Guo, W. Polyethyleneimine modified bentonite for the adsorption of amino black 10B. *J. Solid State Chem.* **2017**, *252*, 152–157. [CrossRef]
30. Sheikhmohammadi, A.; Mohseni, S.M.; khodadadi, R.; Sardar, M.; Abtahi, M.; Mahdavi, S.; Keramati, H.; Dahaghin, Z.; Rezaei, S.; Almasian, M.; et al. Application of graphene oxide modified with 8-hydroxyquinoline for the adsorption of Cr(VI) from wastewater: Optimization, kinetic, thermodynamic and equilibrium studies. *J. Mol. Liq.* **2017**, *233*, 75–88. [CrossRef]
31. El-Dais, F.M.S.E.; Sayed, A.E.O.; Salah, B.A.; Shalabi, M.E.H. Removal of nickel(II) from aqueous solution via carbonized date pits and carbonized rice husks. *Eurasian Chem. J.* **2011**, *13*, 267–277. [CrossRef]
32. Mellah, A.; Chegrouche, S.; Barkat, M. The removal of uranium(VI) from aqueous solutions onto activated carbon: Kinetic and thermodynamic investigations. *J. Colloid Interface Sci.* **2006**, *296*, 434–441. [CrossRef] [PubMed]
33. Wang, Y.Q.; Zhang, Z.B.; Li, Q.; Liu, Y.H. Adsorption of thorium from aqueous solution by $HDTMA^+$-pillared bentonite. *J. Radioanal. Nucl. Chem.* **2012**, *293*, 519–528. [CrossRef]
34. Khalili, F.; Al-Banna, G. Adsorption of uranium(VI) and thorium(IV) by insolubilized humic acid from Ajloun soil—Jordan. *J. Environ. Radioact.* **2015**, *146*, 16–26. [CrossRef] [PubMed]
35. Gao, Y.; Shao, Z.; Xiao, Z. U(VI) sorption on illite: Effect of pH, ionic strength, humic acid and temperature. *J. Radioanal. Nucl. Chem.* **2015**, *303*, 867–876. [CrossRef]
36. Zhang, H.; Wang, X.; Liang, H.; Tan, T.; Wu, W. Adsorption behavior of Th(IV) onto illite: Effect of contact time, pH value, ionic strength, humic acid and temperature. *Appl. Clay Sci.* **2016**, *127–128*, 35–43.
37. Wm, Y. Uranium Adsorption from Aqueous Solution Using Sodium Bentonite Activated Clay. *J. Chem. Eng. Process Technol.* **2017**, *8*, 1–8. [CrossRef]

38. Yin, Z.; Pan, D.; Liu, P.; Wu, H.; Li, Z.; Wu, W. Sorption behavior of thorium(IV) onto activated bentonite. *J. Radioanal. Nucl. Chem.* **2018**, *316*, 301–312. [CrossRef]
39. Zareh, M.M.; Aldaher, A.; Hussein, A.E.M.; Mahfouz, M.G.; Soliman, M. Uranium adsorption from a liquid waste using thermally and chemically modified bentonite. *J. Radioanal. Nucl. Chem.* **2013**, *295*, 1153–1159. [CrossRef]
40. Pan, D.Q.; Fan, Q.H.; Li, P.; Liu, S.P.; Wu, W.S. Sorption of Th(IV) on Na-bentonite: Effects of pH, ionic strength, humic substances and temperature. *Chem. Eng. J.* **2011**, *172*, 898–905. [CrossRef]
41. Wang, J.; Chen, Z.; Shao, D.; Li, Y.; Xu, Z.; Cheng, C.; Asiri, A.M.; Marwani, H.M.; Hu, S. Adsorption of U(VI) on bentonite in simulation environmental conditions. *J. Mol. Liq.* **2017**, *242*, 678–684. [CrossRef]